BOND STRENGTH ANALYSIS IN CONTINUOUS FIBER REINFORCED THERMOPLASTICS

Jiakuan, Zhou[a], Frederik, Desplentere[b], Jan, Ivens[a]

a: KU Leuven, Department of Materials Engineering, Campus De Nayer, Sint-Katelijne-Waver, Belgium – jiakuan.zhou@kuleuven.be
b: KU Leuven, Department of Materials Engineering, Campus Brugge, Brugge, Belgium

Abstract: *Bond strength development is essential in the continuous processing of fiber reinforced thermoplastic laminates. A wedge peel test is an easy to perform test to assess the bond strength development as a function of processing parameters. In this research, compression molded glass fiber reinforce polypropylene (GF/PP) and glass fiber reinforced styrene-acrylonitrile (GF/SAN) unidirectional laminates exemplified the relationship between processing parameters and bond strength by wedge peel tests. Results showed that bond strength was dominated by cooling rate with around 20% (amorphous SAN) to 100% (semicrystalline PP) increase under high cooling rate, together with the effect of fiber interpenetration and interlaminar resin pockets. This was illustrated by failure mode analysis through fracture surface morphology under light microscope and SEM, fiber interpenetration analysis by μCT measurements, and crystallization analysis by XRD. In conclusion, high cooling rate and relaxation time enhance bond strength of continuous fiber reinforced thermoplastics in present research.*

Keywords: Bond strength; Continuous fiber reinforced thermoplastics; Wedge peel test; Fiber interpenetration; Crystallization

1. Introduction

Processing and manufacturing of thermoplastics plus their composites rely on the fusion bonding, which is attained by first intimate contact and then autohesion[1]. And the final product quality is significantly affected by the bond strength development which is a function of processing temperature, pressure and time. The promising automated tape placement (ATP) of continuous fiber reinforced thermoplastics (CFRT) enables digital, efficient, environmentally friendly manufacturing of lightweight and high-performance structures in aeronautics, automotive and wind power industry etc.. However, for such a fast in-situ non-isothermal consolidation process, achieving a high-quality bonding is challenging due to that intimate contact may not completely finish prior to healing, overheating induced thermoplastics degradation etc.[3]. This puts forward demands of an easy and efficient method of bond strength characterization.

The characterization of bond strength is to quantify the interlaminar shear strength of fusion bonded laminates. This is probably the most complicated property to determine as the difficulty of obtaining a uniform and stable stress state. Some standard test methods are widely used, like double cantilever beam (DCB) test[4] (e.g. ASTM D5528), lap shear test[5] (e.g. ASTM D5868), or short beam strength (SBS) test[6] (e.g. ASTM D2344). However, the above mentioned tests normally require a thick bulk laminates, which means relatively long sample preparation time.

Moreover, Schäfer[7] reported that undesired failure mode happened when performing SBS tests on carbon fiber reinforced polyamide 6, and bond strength by lap shear test can be strongly affected by moisture. Instead, some peel tests can be used, like T-peel test[8] (e.g. ASTM D1876), mandrel peel test[9] (e.g. DIN EN 2243) and wedge peel test. For the T-peel test and mandrel peel test, at least one flexural peel arm is prerequisite, and large fluctuation of peel force might occur[10]. The wedge peel test has not been standardized yet, but it's proved that bond strength by wedge peel test is significantly correlated with that by DCB test[11,12], and it's easy to prepare specimens and perform tests in the meanwhile. This makes it suitable for tests on thin laminates like those made by ATP, and a reliable alternative to widely used standard tests.

The present research focuses on the exploration of bond strength development as a function of processing parameters that are decisive for high laminates quality through wedge peel tests. Glass fiber reinforce polypropylene (GF/PP) and glass fiber reinforced styrene-acrylonitrile (GF/SAN) unidirectional (UD) tapes were compression molded into 4-ply laminates under different processing temperatures and cooling rates. Then the bond strength corresponding to different processing parameters were quantified by wedge peel tests, and further analyzed. The difference in bond strength level between GF/PP and GF/SAN was demonstrated by fracture surface morphology under light microscope and SEM. The bond strength comes from fiber interpenetration and waviness between plies was emphasized and quantified by µCT measurements, as this differentiate the bond strength in CFRT from pure polymers. Moreover, the significant bond strength increase in GF/PP under high cooling rate was illustrated by crystallization analysis with X-ray diffraction (XRD).

2. Materials and Experiments

2.1 Materials and sample preparation

Commercial GF/PP UD tapes (UDMAX™ GPP 45-70 TAPE, sourced by FRT Tapes) and GF/SAN UD tapes produced by authors' project partners were selected for the present research. Both of them are 0.25 mm thick. Besides, the melting point (T_m) of semi-crystalline PP is around 166 °C, and the glass transition temperature (T_g) of amorphous SAN is around 102 °C.

Samples for wedge peel tests were manufactured by compression molding, since the processing parameters can be accurately controlled in such a bulk-consolidation process as compared to ATP. Two hot press machines were used for different cooling rate, namely Fontijne lab press – TP 400 and Pinette press zenith 2. First the tapes were cut into 24 cm long ones, and then 4 plies of tapes were stacked together and wrapped by a folded Teflon film between two steel plates, instead of a mold. The Teflon film is 0.15 mm thick, which ensures smooth surface quality and weak constraints like a mold. Another small piece of Teflon film as crack starter, was placed between the second and third ply on one end of the stack, this way a non-bonded area can be obtained for crack initiation. Finally some $[0]_4$ laminate plates were made with Fontijne press and Pinette press separately for each processing setting, and trimmed into 240 mm * 100 mm. Each plate was directly cut along fiber direction, resulting in six wedge peel test specimens that are around 15 mm wide, with two non-bonded free legs for each. Besides, samples for µCT and XRD were cut from the center of the bonded areas.

2.2 Processing parameters

At first the hot press was pre-heated to the designated isothermal temperature, which is from 190 °C, 200 °C to 240 °C for GF/PP, according to the recommended range on the data sheet, and 220 °C, 230 °C as well as 240 °C for GF/SAN. The pressure for all experiments was set to 7 bar for both holding and cooling process. After the hot press stabilized at the isothermal temperature, the stacked tapes together with Teflon film and steel plates were put in the hot press for 10 min holding, at the set temperature and pressure. For the cooling process, samples were forced cooled until the temperature below 30 °C, and then demolded. There are some differences in the cooling between Fontijne press and Pinette press. For the Fontijne press, samples are kept between 2 plate molds with pressure for both holding and cooling process, and the forced cooling is achieved with flow water in plate molds. For the Pinette press, there are separate hot stage and cold stage, and the forced cooling is achieved by transferring samples from hot stage to cold stage that stays at room temperature all the time. As a result, the cooling rate of Pinette is much higher than that of Fontijne press. Besides, it's worth mentioning that the transfer manipulation results in around 20 s pressureless relaxation time for the sample. The temperature profile of whole process was measured by thermocouples inside the stacked tapes, and the approximate cooling rate for Fontijne press and Pinette press is given in Table 1.

Table 1: Approximate cooling rate at specific temperature in the cooling process

	Cooling rate at 200 °C	Cooling rate at 166 °C	Cooling rate at 102 °C
Fontijne samples	51 K/min	42 K/min	23 K/min
Pinette samples	604 K/min	484 K/min	206 K/min

2.3 Wedge peel tests

The present research used the wedge peel test setup mentioned by ref. [7,13]. An aluminum frame is vertically mounted onto the bottom of a static universal testing machine Instron 4467, with a wedge fixed on its top. A 3.2 mm thick wedge was rounded, with an angle of 20° and a radius of 0.5 mm, for a valid failure mode. Two free legs of the tested specimen were put on either side of the wedge, wrapped by a sand paper to prevent slippage, and then clamped by pneumatic grips above the wedge. A 1 kN load cell was used to record the wedge peel force, and 10 data points were sampled per second.

Before starting tests, the specimen width was measured at 3 different locations of the bonded area, and the average value was used as the nominal width. When performing tests, the upper cross-head rose vertically at the speed of 60 mm/min, pulling the specimens upward. Naturally, the wedge cut through the interface and peeled the second and third ply.

3. Results and discussion

3.1 Wedge peel strength

An example of typical wedge peel force – displacement curves is gives in Figure 1. The "F" in legend means Fontijne samples and the "P" means Pinette samples. Due to the running-in effect at the beginning of peeling, the data points before 60 mm were discarded. For each specimen, the selected data points for statistical evaluation ranged from 60 mm to 140 mm, as they were relatively stable. The wedge peel force in this region was averaged, and then normalized by the nominal width of the corresponding specimen, yielding the wedge peel strength.

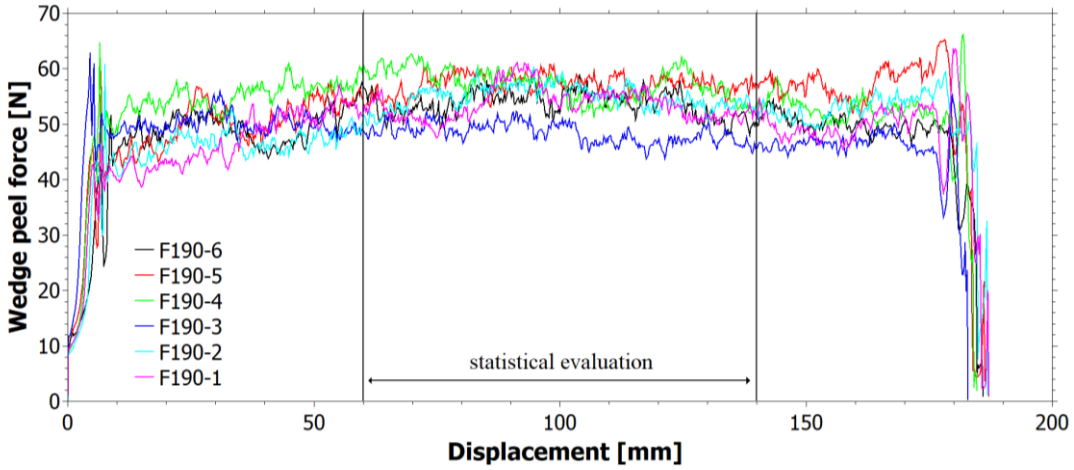

Figure 1. An example of typical wedge peel force – displacement curves for GF/PP Fontijne samples made at 190 °C

The results of the wedge peel strength is presented in Figure 2. All the GF/PP samples show a higher level of wedge peel strength than GF/SAN samples, no matter they were made by Fontijne press or Pinette press. Moreover, there is a significant difference in the increase of wedge peel strength from low cooling rate to high cooling rate. Specifically, wedge peel strength of Pinette samples is 100% and 20% higher than Fontijne samples for GF/PP and GF/SAN respectively. However, wedge peel strength for both GF/PP and GF/SAN is not sensitive towards the set processing temperatures, as it keeps at a close level for the same material and the same hot press machine.

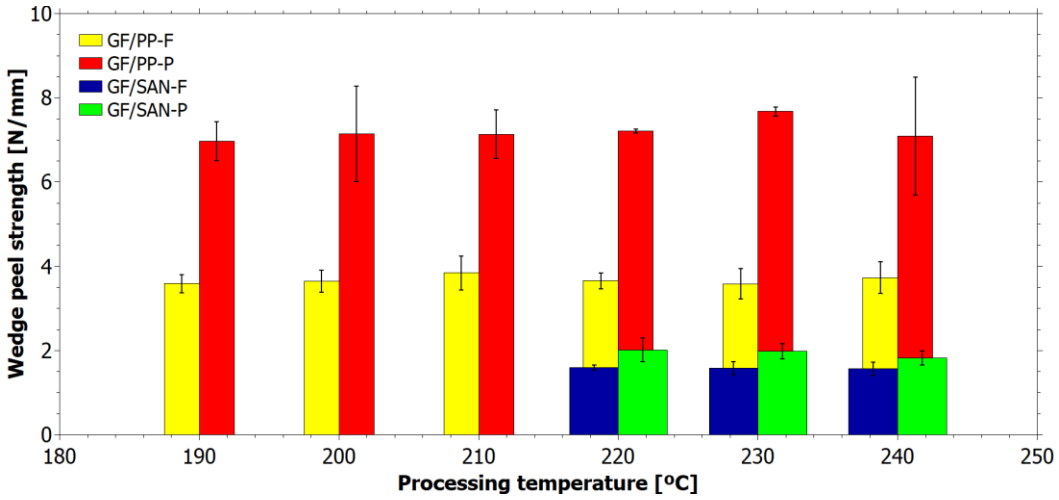

Figure 2. Wedge peel strength of both GF/PP and GF/SAN samples

3.2 Light microscopy and scanning electron microscopy

The delaminated surfaces were observed. Light microscopy showed fibers were pulled out for both GF/PP and GF/SAN, which indicated that there were fibers of one ply interpenetrated into the adjacent ply. Besides, stress whitening phenomenon was also found on PP matrix. The interpenetrated fibers worked like entangled polymer chains while even stiffer, diverting some strain energy from the crack tip and increasing the interlaminar toughness. A further observation on pulled-out fibers was done under SEM, see Figure 3. It shows that resin was still tightly

adhered and wrapped on pulled-out fibers for GF/PP but not for GF/SAN. All these morphologies illustrate different failure modes (plastic yielding with stress whitening, cohesive failure for GF/PP, while brittle damage and fiber-matrix interfacial failure for GF/SAN), and explain the much higher bond strength of GF/PP as compared to GF/SAN.

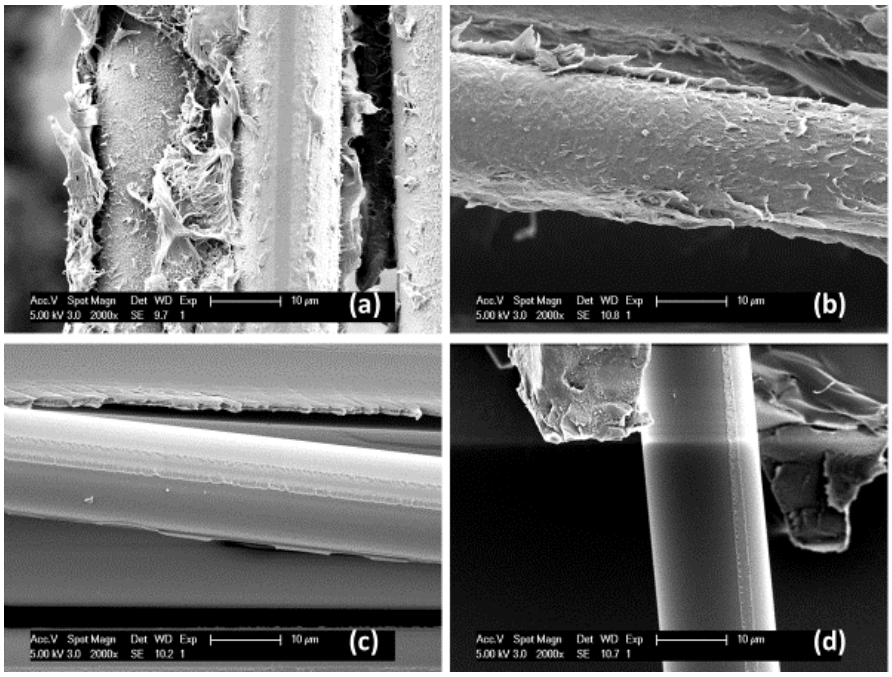

Figure 3. Pulled-out fibers of (a) GF/PP-F, (b) GF/PP-P, (c) GF/SAN-F and (d) GF/SAN-P under SEM

The cross-sections of compression molded laminates were also observed with light microscope as presented in Figure 4. It's obvious that Pinette samples have more inhomogeneous fiber distribution and more resin pockets at the interfaces, possibly due to capillary percolation during pressureless relaxation time. This contributes to the higher bond strength of Pinette samples as the bond strength is polymer matrix dominating.

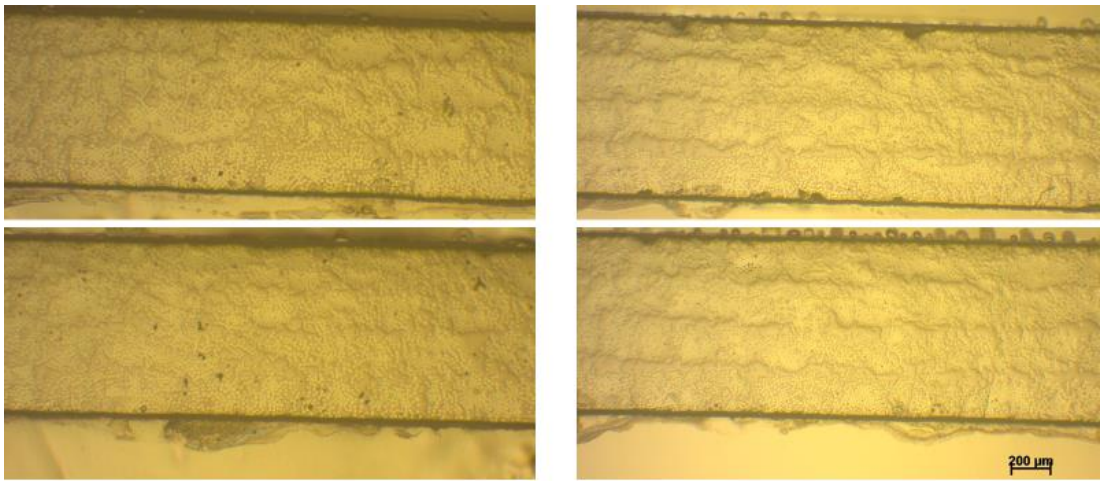

Figure 4. Cross-sections of GF/PP-F240 on the left and GF/PP-P240 on the right as examples

3.3 µCT measurement

The classical bond strength development theory by Yang and Pitchumani[1] considered fusion bonding between 2 pure polymer substrates. However, the materials in present research are thermoplastics reinforced by fibers. Although the bond strength between 2 CFRT tapes is still dominated by polymer matrix, fiber interpenetration as mentioned above, should also be considered. The interpenetrated fibers differ from their counterparts on the orientation, which will be reflected by the deviation of fiber's orientation angles. This was analyzed on VoxTex developed by the authors' group[14], with corresponding µCT data.

Multi-scan (5 scans with 10 mm intervals) was performed on each sample with same X-ray parameters and voxel size. The µCT images showed similar cross-section morphology with micrographs presented in Figure 4. Then the orientation analysis were performed on VoxTex with the YZ plane (parallel to the laminate surface) as the projection plane, yielding the orientation distribution functions of in-plane angle φ and the out-of-plane angle θ. The root mean square value (RMS) of φ and θ was chosen as an indicator for the comparison of fiber interpenetration and waviness, and RMSs of 5 scans were averaged as the RMS of that sample, as presented in Table 2. It's clear that both RMS of φ and θ of Pinette samples are higher than those of Fontijne samples, which reflects the higher degree of interpenetration and (in-plane) waviness for Pinette samples. This is also attributed to the pressureless relaxation time.

Table 2: RMS values of fiber orientation angles for all GF/PP and GF/SAN samples

Sample	RMS of φ	RMS of θ	Sample	RMS of φ	RMS of θ
GF/PP-F200	0,8282	0,4120	GF/PP-P200	1,3202	0,4592
GF/PP-F210	0,8771	0,4342	GF/PP-P210	1,0619	0,4616
GF/PP-F220	0,9297	0,4187	GF/PP-P220	1,6568	0,5756
GF/PP-F230	1,3678	0,4622	GF/PP-P230	1,4708	0,5348
GF/PP-F240	1,0495	0,4263	GF/PP-P240	1,3086	0,4998
GF/SAN-F220	0,9885	0,4322	GF/SAN-P220	1,6860	0,8468
GF/SAN-F230	1,1750	0,5420	GF/SAN-P230	1,4230	0,6816
GF/SAN-F240	1,2434	0,4972	GF/SAN-P240	1,3772	0,6804

3.4 X-ray diffraction

However, fiber interpenetration and interlaminar resin pockets cannot totally explain the giant differences in strength increase between GF/PP (~100%) and GF/SAN (~20%) by Pinette press compared with them by Fontijne press. As bond strength is highly dominated by matrix, a critical difference, that PP is semi-crystalline while SAN is amorphous, should be investigated. As the crystallization of PP may play a significant role, the XRD measurements were performed with 2θ range from 5° to 60° and a step length of 0.02°. The measured XRD patterns are showed in Figure 5. The strongest crystal peaks located at 2θ of around 14.1°, 16.9°, 18.6°, 21.1° and 21.9°, as well as some small peaks afterwards, represent the α – PP which exists in both Fontijne samples and Pinette samples. However, another small peak marked by black arrow at 2θ of around 16.2° demonstrates the existence of β – PP in Pinette samples. Differential scanning calorimetry (DSC) results also support the this, but wouldn't be discussed here due to paper length limitation.

Next, further crystallization analysis was done through profile fitting on Jade. The crystallinity X_c and the crystallite size X_s can be seen from Table 3 and 4 respectively. It's clear that for Pinette

samples, high cooling rate induced lower crystallinity, smaller crystallite size and β-crystals. The fine α – PP and β – PP exhibit higher ductility, significantly enhancing the bond strength of GF/PP.

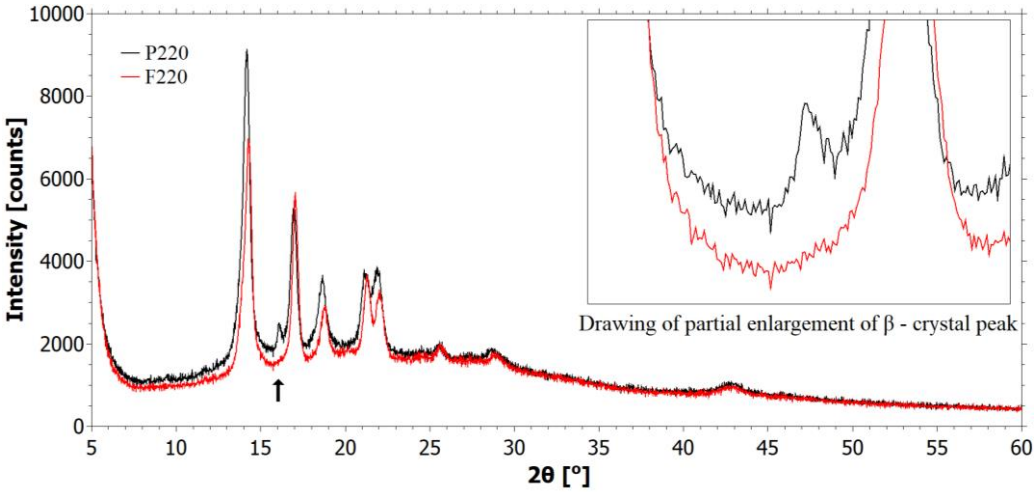

Figure 5. Typical XRD patterns of GF/PP, with F220 and P220 as examples

Table 3: Crystallinity X_c of GF/PP samples made at set temperatures

	Crystallinity X_c of GF/PP made at set temperatures					
	190 °C	210 °C	220 °C	230 °C	240 °C	250 °C
Fontijne samples	49,79%	48,21%	47,07%	50,20%	49,45%	49,98%
Pinette samples	40,93%	42,21%	41,07%	42,21%	40,89%	41,29%

Table 4: Average crystallite size X_s of GF/PP samples made by Fontijne and Pinette press

	Average X_s [Å] of α – PP crystals at different 2θ				
	14,14°	16,87°	18,58°	21,11°	21,86°
Fontijne samples	165,17	221,83	195	185,83	168,33
Pinette samples	167,67	207,17	162,17	144,17	145,33

4. Conclusion

In this paper, wedge peel tests were performed on GF/PP and GF/SAN laminates to characterize their bond strength. Results showed that bond strength was dominated by cooling rate with around 20% (amorphous SAN) to 100% (semicrystalline PP) increase under high cooling rate. Different failure modes explain the higher bond strength of GF/PP in general. The pressureless transfer of laminates from the hot stage to the cold stage induced interlaminar resin pockets and fiber interpenetration between plies, which contributes the minor part (20%) of bond strength increase for both materials. The major part (80%) of the increase for semicrystalline GF/PP relies on crystallization effects, as the lower crystallinity, smaller crystallite size and existence of β-crystals under high cooling rate resulted in more ductile PP matrix. In conclusion, high cooling rate and relaxation time enhance bond strength of CFRT in present research.

In the future, some more works on the quantitative relation between degree of fiber interpenetration and bond strength is promising. Regarding the wedge peel test, the

compression molded laminates can be used as reference materials that already reach 100% degree of bond, and then the degree of bonding for the same materials by the same or other processing techniques as well as processing parameters can be estimated on this basis. Besides, the effects of friction force, wedge geometry, and test parameters like cross-head speed etc. on wedge peel tests deserve further investigation.

Acknowledgements

The present research was supported by ProUD project.

5. References

1. Yang F, Pitchumani R. Nonisothermal healing and interlaminar bond strength evolution during thermoplastic matrix composites processing. Polym Compos. 2003;24(2):263–78.
2. Butler CA, Mccullough RL, Pitchumani R, Gillespie Jr JW. An analysis of mechanisms governing fusion bonding of thermoplastic composites. J Thermoplast Compos Mater. 1998;11(4):338–63.
3. Tierney J, Gillespie Jr JW. Modeling of in situ strength development for the thermoplastic composite tow placement process. J Compos Mater. 2006;40(16):1487–506.
4. Ray D, Comer AJ, Lyons J, Obande W, Jones D, Higgins RMO, et al. Fracture toughness of carbon fiber/polyether ether ketone composites manufactured by autoclave and laser-assisted automated tape placement. J Appl Polym Sci. 2015;132(11).
5. Qureshi Z, Swait T, Scaife R, El-Dessouky HM. In situ consolidation of thermoplastic prepreg tape using automated tape placement technology: Potential and possibilities. Compos Part B Eng. 2014;66:255–67.
6. Carlsson LA, Adams DF, Pipes RB. Basic experimental characterization of polymer matrix composite materials. Polym Rev. 2013;53(2):277–302.
7. Schäfer PM. Consolidation of carbon fiber reinforced polyamide 6 tapes using laser-assisted tape placement. Technische Universität München; 2017.
8. Awaja F. Autohesion of polymers. Polymer (Guildf). 2016;97:387–407.
9. Marinosci VM, Grouve WJB, de Rooij MB, Wijskamp S, Akkerman R. Effect of grit-blasting on the fracture toughness of hybrid titanium-thermoplastic composite joints. Int J Adhes Adhes. 2021;109:102893.
10. Boiko YM, Lyngaae-Jørgensen J. Fracture energy–fracture stress relationship for weak polymer–polymer interfaces. Polymer (Guildf) [Internet]. 2005;46(16):6016–24.
11. Hulcher B, Marchello JM, Hinkley JA. Correlation between double cantilever beam and wedge peel tests for automated tow placement. Mater Process affordability- Keys to Futur. 1998;1955–65.
12. Hulcher AB, Marchello JM, Hinkley JA. Wedge peel testing for automated fiber placement. J Adv Mater. 1999;31(3):37–43.
13. Stokes-Griffin CM, Kollmannsberger A, Compston P, Drechsler K. The effect of processing temperature on wedge peel strength of CF/PA 6 laminates manufactured in a laser tape placement process. Compos Part A Appl Sci Manuf. 2019;121:84–91.
14. Straumit I, Lomov S V, Wevers M. Quantification of the internal structure and automatic generation of voxel models of textile composites from X-ray computed tomography data. Compos Part A Appl Sci Manuf. 2015;69:150–8.

